Available online at www.sciencedirect.com
ScienceDirect
Engineering Fracture Mechanics 75 (2008) 1251–1265
Engineering Fracture Mechanics
www.elsevier.com/locate/engfracmech

Evaluation of polymer fracture parameters by the boundary element method

Stavros Syngellakis [a,*], Jiangwei Wu [b]

[a] School of Engineering Sciences, University of Southampton, Southampton SO17 1BJ, UK
[b] Department of Mechanical Engineering, Shanghai Maritime University, 1550 Pu Dong Avenue, Shanghai 200135, PR China

Received 15 August 2006; received in revised form 27 March 2007; accepted 3 April 2007
Available online 18 April 2007

Abstract

The boundary element method (BEM) for two-dimensional linear viscoelasticity is applied to polymer fracture. The time-dependence of stress intensity factors is assessed for various viscoelastic models as well as loading and support conditions. Various representations of the energy release rate under isothermal conditions are adopted. Additional boundary integral equations for the displacement gradient in the domain are linked to algorithms for the evaluation of path-independent J-integrals. The consistency of BEM predictions and their good agreement with other analytical results confirms BEM as a valid modelling tool for viscoelastic fracture characterisation and failure assessment under complex geometric and loading conditions.

Keywords: Viscoelasticity; Energy release rate; J-integral; Boundary element method

1. Introduction

The increasing use of polymers has prompted extensive research on their failure mechanisms. Polymer fracture, in particular, has been the subject of many theoretical studies concerned with the identification and determination of parameters governing crack initiation and growth. For a linear viscoelastic solid, the time-dependent solutions for the stress and displacement fields near the tip of stationary crack can be produced by applying the elastic–viscoelastic correspondence principle [1]. The stress intensity factor K_I and the crack-opening displacement can be easily deduced from such solutions. When viscoelastic materials with constant Poisson's ratio are subjected to constant traction, K_I remains constant in time. Even in such cases however, the energy release rate G is time-dependent in common with other properties, such as relaxation modulus and creep compliance. Therefore, a critical strain energy release rate $G_C(t)$ is considered as the characterising parameter for crack extension rather than the fracture toughness K_{IC} [2]. Under certain conditions,

* Corresponding author. Tel.: +44 23 80592844; fax: +44 23 80594813.
E-mail address: ss@soton.ac.uk (S. Syngellakis).

0013-7944/$ - see front matter © 2007 Elsevier Ltd. All rights reserved.
doi:10.1016/j.engfracmech.2007.04.009

Nomenclature

a	half crack length
b	cracked plate depth
C	compliance function
c	crack propagation velocity
E	uni-axial relaxation modulus
e_{ij}	deviatoric strains
G	energy release rate
H	Heaviside step function
K_{I}	mode I stress intensity factor
k	bulk relaxation function
p_i	traction
$\tilde{p}_i$	applied traction
r, θ	polar co-ordinates with origin at crack tip
s	Laplace transform parameter
s_{ij}	deviatoric stresses
t, τ	time
U_s	surface energy stored
W	strain energy
w	cracked plate length
u_i	displacement
$\tilde{u}_i$	applied displacement
x_i	Cartesian co-ordinates ($i = 1, 2$)
Γ	cracked plate boundary
Γ_J	J-integral contour
Γ_{p}	traction-loaded plate boundary
Γ_{u}	displacement-loaded plate boundary
δ_{ij}	Kronecker delta
ε_{ij}	strains
κ	1 for plane stress, $1 - \nu^2$ for plane strain
μ	shear relaxation function
ν	Poisson's ratio
σ_{ij}	stresses
$\hat{\sigma}^I_{ij}$	non-singular part of near-tipstresses (mode I)
Ω	cracked plate domain

the path-independent J-integral, defined by Rice [3] for elastic materials, is shown to be equivalent to the energy release rate.

Although many theoretical and experimental studies on viscoelastic fracture behaviour can be found in the literature [2,4–7], numerical applications in this area are relatively limited. The time-dependent aspects of fracture in polymers are discussed in a review by Knauss [8]. Only a few papers reported the analysis of linear viscoelastic fracture behaviour using numerical methods. Applications of the finite element method in this area [9] have been mainly concerned with simulations of fracture behaviour in polymer matrix composites. Relatively few attempts have been made to predict material parameters characterising fracture behaviour.

The application of the boundary element method (BEM) to polymer fracture has been even rarer. An early such solution [10], based on the Laplace transform approach, predicted the crack-opening displacement of a penny-shaped crack in a viscoelastic material characterised by a three-parameter Kelvin model. Two-dimensional stress and displacement fields were later analysed in the neighbourhood of a crack filled with failed, so-called craze material [11]. More recently, a direct, time-domain BEM formulation was applied to the

evaluation of an expression for the strain energy release rate derived from a functional corresponding to the potential energy in elasticity [12]. Further results have confirmed the effectiveness of both Laplace transform and time-domain BEM in predicting time-dependent stress intensity factors and energy release rates under constant loads [13].

The present BEM analysis attempts to provide a general theoretical framework for generating key fracture parameters under any time-dependent loading. Linear viscoelasticity, the most commonly adopted model for polymers, has been assumed. Various approaches for representing the energy release rate or crack extension force under isothermal conditions have been adopted. Additional boundary integral equations have been derived for the displacement gradient distributions in the solid domain leading to algorithms for the evaluation of path-independent J-integrals. The developed analysis procedure includes an assessment of the crack growth rate based on the knowledge of the critical energy release rate and an energy balance equation.

Computer codes for both Laplace transform and time-domain analyses under both plane stress and plane strain conditions have been developed and applied initially to the prediction of near crack-tip stress and crack-opening displacement time histories in centre-cracked specimens under tension in order to assess their relative accuracy and efficiency. The time-dependence of stress intensity factors is assessed for various viscoelastic models as well as loading and support conditions. Numerical results have also been obtained for the energy release rate under constant strain and constant strain rate loading. Geometric and material input has been linked to specimens from published reports of experimental investigations. BEM predictions are compared with other analytical results; their consistency with theoretical expectations and experimental observations is also examined.

2. Viscoelastic fracture mechanics

The analysis is applied to a plate with a straight central crack of length $2a$ as shown in Fig. 1, where Ω and Γ represent the plate domain and boundary, respectively. The plate is subjected to quasi-static, time-dependent combinations of edge displacement $\tilde{u}_i(t)$ on Γ_u and traction $\tilde{p}_i(t)$ on Γ_p with $\Gamma_u \cup \Gamma_p = \Gamma$. Both geometry and loading are assumed symmetric relative to the co-ordinate axes x_i $(i = 1,2)$, parallel and perpendicular to the crack with origin at its centre. The loading results in crack opening mode I, and the crack tip is defined according to Schapery [4], that is, accounting for a failure zone between crack surfaces. As pointed out in the previous section, the material is assumed linear, isotropic, viscoelastic for which the constitutive relations

$$s_{ij} = 2\mu(t)e_{ij}(0) + 2\int_0^t \mu(t-\tau)\frac{\partial e_{ij}(\tau)}{\partial \tau}\mathrm{d}\tau \tag{1}$$

$$\sigma_{kk} = 3k(t)\varepsilon_{kk}(0) + 3\int_0^t k(t-\tau)\frac{\partial \varepsilon_{kk}(\tau)}{\partial \tau}\mathrm{d}\tau \tag{2}$$

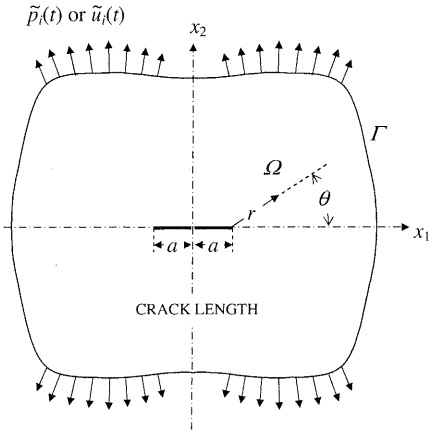

Fig. 1. Schematic representation of a centre-cracked plate.

apply, where σ_{ij} are the stresses, ε_{ij} the strains, s_{ij}, e_{ij} represent the deviatoric stresses and strains, respectively defined as

$$s_{ij} = \sigma_{ij} - \frac{1}{3}\sigma_{kk}\delta_{ij}, \quad e_{ij} = \varepsilon_{ij} - \frac{1}{3}\varepsilon_{kk}\delta_{ij} \tag{3}$$

and δ_{ij} is the Kronecker delta. In Eqs. (1) and (2), $\mu(t)$ and $k(t)$ are the shear and bulk relaxation functions, respectively while repeated indices represent summation over their range. Adopting the notation

$$\phi * \mathrm{d}\psi = \psi * \mathrm{d}\phi = \phi(t)\psi(0) + \int_0^t \phi(t-\tau)\frac{\partial\psi(\tau)}{\partial\tau}\mathrm{d}\tau$$

for the Stieltjes convolution of two functions ϕ and ψ, the constitutive relations (1) and (2) can be written

$$s_{ij} = 2\mu * e_{ij}, \quad \sigma_{kk} = 3k * \varepsilon_{kk}.$$

2.1. Stress intensity factor

In the neighbourhood of the crack tip, the stress field is given, relative to a local polar frame of reference (r, θ), by the time-domain relations

$$\sigma_{ij}(r,\theta,t) = \frac{K_{\mathrm{I}}(t)}{\sqrt{2\pi r}}\hat{\sigma}^{\mathrm{I}}_{ij}(\theta), \tag{4}$$

where K_{I} is the mode-I, time-dependent stress intensity factor for the cracked plate of Fig. 1 and $\hat{\sigma}^{\mathrm{I}}_{ij}$ are known functions of θ. If the time-domain solution for the stress field is known, K_{I} can be directly calculated using

$$K_{\mathrm{I}}(t) = \lim_{r\to 0}\sigma_{22}(r,0,t)\sqrt{2\pi r}. \tag{5}$$

The stress intensity factor depends, in general, on both the loading and the viscoelastic properties [14]. In the special case of separation of variables conditions, that is, for constant Poisson's ratio, the stress field depends only on the loading history, therefore, K_{I} can be obtained by applying the correspondence principle. The Laplace transform of Eq. (4) yields the relations [15]

$$\bar{\sigma}_{ij}(r,\theta,s) = \frac{\bar{K}_{\mathrm{I}}(s)}{\sqrt{2\pi r}}\hat{\sigma}^{\mathrm{I}}_{ij}(\theta) \tag{6}$$

close to the crack tip, where s is the Laplace transform parameter. It was shown [14] that, in the transformed domain, a J-type, path-independent integral can be defined as

$$J_{\mathrm{v}} = \int_{\Gamma_J}\left(\frac{1}{2}\bar{\sigma}_{ij}\bar{\varepsilon}_{ij}\mathrm{d}x_2 - \bar{p}_i\frac{\partial\bar{u}_i}{\partial x_1}\mathrm{d}\Gamma\right), \tag{7}$$

where Γ_J is a contour surrounding the crack tip. The Laplace transform of the stress intensity factor $\bar{K}_{\mathrm{I}}(s)$ is related to J_{v} by

$$J_{\mathrm{v}} = \kappa\frac{\bar{K}^2_{\mathrm{I}}(s)}{E_{\mathrm{v}}}, \tag{8}$$

where κ is equal to 1 or $1-\nu_{\mathrm{v}}^2$ for plane stress or plane strain, respectively and

$$E_{\mathrm{v}} = s\bar{E} = \frac{9s\bar{k}\bar{\mu}}{3\bar{k}+\bar{\mu}}, \quad \nu_{\mathrm{v}} = s\bar{\nu} = \frac{3\bar{k}-2\bar{\mu}}{2(3\bar{k}+\bar{\mu})}, \tag{9}$$

where $E(t)$ is the uniaxial relaxation modulus and $\nu(t)$ the Poisson's ratio.

2.2. Energy release rate

The crack is initially assumed to be stationary until time $t = t_1$, when it is forced to grow by a small amount δa in order to assess the corresponding rate of energy release. This crack extension is equivalent to the removal

of the tension $p_2(x_1,0,t)$ for $a \leqslant x_1 \leqslant a+\delta a$ and $t \geqslant t_1$. According to the principle of superposition, the response of the plate with a crack length $a+\delta a$ can be obtained by adding to the original solution a new incremental viscoelastic solution performed with tension $p_2(x_1,0,t)$ reversed, that is, applied as compression on the extended crack surface, with boundary conditions $\tilde{u}_i(t)=0$ on $\Gamma_u, \tilde{p}_i(t)=0$ on Γ_p and effective moduli $\mu(t-t_1)$ and $k(t-t_1)$.

Energy conservation requires [16,17]

$$\int_\Gamma p_i \frac{\partial u_i}{\partial a} d\Gamma = \frac{\partial}{\partial a}\int_\Gamma \int_0^{\delta u_i(t')} p_i du_i d\Gamma + \frac{2}{\delta a}\int_0^{\delta a} dr \int_0^{u_2(t')} p_2 du_2, \tag{10}$$

where $t' = t - t_1$. The left-hand side in Eq. (10) represents the rate of input energy while, on the right-hand side, the first term is the rate of energy stored including energy dissipation and the second the energy release rate at the crack tip due to the crack opening displacement $2u_2(r,t')$. Noting that the changes in energy are associated with the incremental solution, Eq. (10) can lead directly to an estimate of the energy release rate $G(t)$, which is defined as

$$G = \int_\Gamma p_i \frac{\partial u_i}{\partial a} d\Gamma - \frac{\partial}{\partial a}\int_\Gamma \int_0^{\delta u_i} p_i du_i d\Gamma = \frac{\partial U_s}{\partial a}, \tag{11}$$

where U_s is the surface energy stored. Thus, comparing Eqs. (10) and (11) gives

$$G = \frac{\partial U_s}{\partial a} = \frac{2}{\delta a}\int_0^{\delta a} dr \int_0^{u_2(t')} p_2 du_2. \tag{12}$$

The evaluation of the integral

$$\int_0^{u_2(t')} p_2 du_2 \tag{13}$$

requires knowledge of the function $p_2(u_2,t')$, which is generally nonlinear since it depends on the loading history. This can be built numerically for any given time t' by assuming a relation

$$u_2(t') = C(r,t')p_2(0) + \int_0^{t'} C(r,t'-\tau)dp_2, \tag{14}$$

where the compliance function $C(r, t')$ depends implicitly on the viscoelastic properties of the material and can be generated numerically for any $r \leqslant \delta a$ from the incremental solution with constant p_2 as the applied load. Thus, the displacement at any intermediate time t_k due to a loading history from $p_2(0)$ to $p_2(t_k)$, can be obtained from Eq. (14) as

$$u_2(t',t_k) = C(t')p_2(0) + \int_0^{t_k} C(t'-\tau)dp_2 \tag{15}$$

yielding pairs of values for $p_i(t_k)$, $u_i(t',t_k)$ for a number of distinct times t_k in the interval from 0 to t'. The energy release rate can thus be calculated at any time t' from Eq. (12), which is valid for any linear viscoelastic material under any loading history. This time-dependent $G(a,t)$, obtained for $t_1 = 0$, corresponds to Williams's definition of parameter J for viscoelastic materials [17]. This notation is here reserved only for the J-integral. At initiation, G reaches a critical value G_C, which is physically interpreted as the upper limit to the fracture resistance of the material [17].

It is of interest to consider the value of G at $t = t_1$, that is, the time of crack extension, when the instantaneous response of the material to $p_2(t_1)$ would be purely elastic characterised by the initial values of the viscoelastic moduli. Then, Eq. (12) reduces to

$$G(a,t_1)\delta a = \int_0^{\delta a} p_2(r,t_1)u_2(r,t_1)dr. \tag{16}$$

The instantaneous energy release rate obtained from Eq. (16), which can be expressed as a function of t_1, is consistent with parameter G as defined by Williams [17] for purely elastic processes.

It is also evident from Eq. (16) that the problem of determining $G(a,t_1)$ is equivalent to that for an elastic material under stresses $\sigma_{ij}(t_1)$, in equilibrium with the applied boundary loading $\tilde{u}_i(t_1)$ and $\tilde{p}_i(t_1)$, characterised by a shear modulus $\mu(0)$ and a bulk modulus $k(0)$. Crack extension to $a+\delta a$ should have the same effect on this state as the removal of $p_2(t_1)$. The stress and traction fields at $t=t_1$ are thus complemented by virtual elastic displacements u_i^R and strains ε_{ij}^R obtained for the real tractions $p_i(t_1)$ using the initial relaxation moduli as the elastic constants. Thus, an alternative means of obtaining $G(a,\ t_1)$ is generated from Eq. (11) which is reduced to

$$G(a,t_1)\delta a = \int_{\Gamma_p} \tilde{p}_i \delta u_i^R \mathrm{d}\Gamma - \frac{1}{2}\delta \int_{\Gamma} p_i u_i^R \mathrm{d}\Gamma. \tag{17}$$

2.3. J-integral

When the evaluation of the strain energy release rate G is based on energy changes from an instantaneously elastic state, a correspondence can be established between the viscoelastic and a fictitious elastic problem. As pointed out by Schapery [2], it would then be possible to identify a path-independent integral $J(t)$ which is identical to G and obtained directly from an elastic solution consisting of the current stress field $\sigma_{ij}(t)$ as well as suitably defined displacements u_i^R and strains ε_{ij}^R fields. Then the path-independent integral is given by [3]

$$J = \int_{\Gamma_J} (W\mathrm{d}x_2 - p_i u_i^R{}_{,1}\mathrm{d}\Gamma), \tag{18}$$

where

$$W = \int_0^{\varepsilon_{ij}^R} \sigma_{ij}(t)\mathrm{d}\varepsilon_{ij}^R. \tag{19}$$

It is always possible to identify $J(t_1)$, corresponding to $G(t_1)$, when the resulting stress field $\sigma_{ij}(t_1)$ is combined with u_i^R and ε_{ij}^R fields, determined from an elastic analysis under boundary traction $p_i(t_1)$, using as material constants the moduli $\mu(0)$ and $k(0)$.

2.4. Crack propagation velocity

The crack will grow when $G(a,t)$ is greater than a constant critical G_C for the material. Then, for a crack extension δa, the excess surface energy will be dissipated as viscoelastic deformation taking place within a time increment δt. The incremental solution should therefore be viscoelastic accounting for the time-dependence of material properties within this interval. The equation of energy equilibrium is thus written [16]

$$G_C \delta a = 2\int_0^{\delta t} \mathrm{d}\tau \int_0^{\delta a} p_2(r,\tau)\dot{u}_2 \mathrm{d}r. \tag{20}$$

An iterative, trial-and-error process generates the value of δt for which Eq. (20) is satisfied. Then, the velocity of crack propagation will be obtained as

$$c = \frac{\delta a}{\delta t}. \tag{21}$$

3. Boundary element modelling

The viscoelastic analysis is performed here numerically using the boundary element method (BEM). There are advantages in applying this method to fracture problems. It has been shown that critical parameters characterising fracture behaviour can be evaluated from known boundary displacements and tractions. If internal variables are required, as in the case of J-integral calculations, these can be evaluated along any contour and for any point density whatever the boundary element mesh. Particular attention is given to the boundary modelling around the crack tip so that the stresses in this region are approximated with reasonable accuracy.

BEM formulations of the linear viscoelastic problem [18] have been recently assessed for efficiency and accuracy in the case of quasi-static loading [19]. Two established approaches, applied here to the analysis of cracked plates, are briefly described next.

3.1. Laplace transform domain

The correspondence principle allows the transformation of a linear viscoelastic problem into an equivalent elastic one governed by the boundary integral equation [19]

$$\kappa_{ij}\bar{u}_i = \int_\Gamma \left[\bar{p}_i(s)u^*_{ij}(s) - \bar{u}_i(s)p^*_{ij}(s)\right]\mathrm{d}\Gamma, \tag{22}$$

where $\bar{u}_i, \bar{p}_i$ are respectively, the Laplace transforms of displacement and traction; u^*_{ij}, p^*_{ij} are the fundamental solutions of the corresponding elastic problem for displacements and tractions in which however, the elastic constants have been replaced by material functions of s obtained by transforming the viscoelastic constitutive Eqs. (1) and (2); $\kappa_{ij} = 0.5\delta_{ij}$ in the case of a smooth boundary. The Laplace transforms of any variable can be evaluated at any number of internal domain points using integral equations similar to Eq. (22). The numerical algorithm for implementing Eq. (22) is the same as that for the corresponding elastic problem, which has been well documented in the literature. The time-dependent response has been determined by Schapery's numerical inversion method [20]. Complex viscoelastic models can be easily accommodated in the fundamental solutions, which can be chosen to satisfy the traction-free conditions over the crack surface [21].

3.2. Time domain

Solutions can alternatively be obtained through time-domain BEM formulations derived from viscoelastic reciprocity relations using fundamental solutions specific to the viscoelastic model used [22]. The boundary integral equation takes the form [19]

$$\kappa_{ij}u_i(t) = \int_\Gamma (u^*_{ij} * \mathrm{d}p_i - p^*_{ij} * \mathrm{d}u_i)\mathrm{d}\Gamma, \tag{23}$$

where the time-dependent fundamental solution $u^*_{ij}(\mathbf{x} - \boldsymbol{\xi}, t)$, satisfying the field equations in an infinite domain, is due to body force

$$F^*_i = \delta_{ij}\delta(\mathbf{x} - \boldsymbol{\xi})H(t), \tag{24}$$

where $\delta(\boldsymbol{x} - \boldsymbol{\xi})$ is the delta function and $H(t)$ the Heaviside step function. Applying the correspondence principle, $u^*_{ij}(\mathbf{x} - \boldsymbol{\xi}, t)$ is obtained as the inverse transform of the fundamental solution of the Laplace transformed problem divided by the transform space parameter s. Such an operation has been carried out in several special cases involving standard linear solid (SLS) creep or relaxation models. A general procedure for deriving the time-dependent fundamental solution was devised for shear and bulk relaxation functions in the form of Prony series. Details of the respective numerical algorithms can be found in earlier publications [18,19].

3.3. Application to fracture problems

In BEM studies of linear elastic fracture behaviour, several different techniques were used in order to deal with the stress singularity at the crack tip. In two dimensions, a cubic boundary element model was applied to the surface geometry of an edge crack [23]. The same problem was solved using a modified fundamental solution, which accounted for a flat, traction-free crack [21]. This method however, cannot be extended to three-dimensional problems. Modelling the singular field for point force acting at the crack tip and using an explicit expression (valid near the tip) for this field, Aliabadi et al. [24] obviated the need for detailed modelling in the vicinity of the crack tip.

The application of special techniques for modelling the stress singularity at the crack tip is avoided here by adopting the constant or discontinuous linear element models. Effective BEM modelling is achieved through

the use of very small such elements near the crack tip. For the constant element model, the node is taken at the middle point of the element. For the discontinuous linear element model, the element has two internal nodes.

The stress intensity factor can be calculated either directly from the stress field near the tip or through the calculation of the J – integral as usually done in FEM applications. From Eq. (18) it is easily seen that to calculate the J-integral, the displacement gradients are required along the path Γ_J. These gradients can be obtained by differentiating the elastic equivalent to the boundary integral Eq. (23) with the source point in the domain,

$$u^{\mathrm{R}}_{j,k} = \int_{\Gamma} (u^{*}_{ij,k} p^{\mathrm{R}}_{i} - p^{*}_{ij,k} u^{\mathrm{R}}_{i}) \mathrm{d}\Gamma. \tag{25}$$

The various numerical algorithms for both Laplace transform and time-domain analyses were implemented through suites of FORTRAN programs specifically developed by the authors for that purpose.

3.4. Validation of elastic fracture analysis

Before applying the present BEM modelling of the fracture problem to a viscoelastic material, its effectiveness and accuracy was examined through the analysis of a classical elastic problem with an established theoretical solution. This is the case of a rectangular plate with a central crack under nominally uniform tension in the direction perpendicular to the crack surfaces. Due to the symmetry of the problem only the analysed quarter of the plate is shown in Fig. 2. The numerical values used in this example are: plate width $w = 11.3$ mm, crack half-length $a = 1$ mm, plate half-depth $b = 10$ mm and $\tilde{p}_2 = 10$ MPa. The shear modulus μ and the Poisson's ratio ν of the material were taken equal to 94.5 GPa and 0.1, respectively.

The constant element model with variable element length was used with the smaller elements located in the neighbourhood of the crack tip. Various meshes were adopted in order to assess the effect of the number of the elements and the element length on the accuracy of the results. It was noted that a smooth variation of element length starting from the crack tip improves significantly the performance of the numerical algorithm. Also the number of the elements was increased to a certain limit beyond which no significant improvement in accuracy was achieved. This limit was linked to the more demanding requirement for accuracy and stability of the J-integral. Fig. 3 shows the final optimum mesh of this problem consisting of 432 boundary elements. The smallest element length was 0.0002 mm, which was the length of the two elements adjacent to the crack tip.

The theoretical values of K_{I} and J-integral for this problem are 17.7820 N/mm$^{3/2}$ and 1.5057 J/m^2, respectively. A semi-circular integration path was adopted as shown in Fig. 2. The J-integral was evaluated for various positions of the path centre and values of the path radius. Stable values were obtained for a range of radii confirming the path-independence of the integral. The most accurate results were found with paths centred at $x = 1$ mm, that is, at the crack tip. The average of these J-integral values was 1.5256 J/m^2; this was taken as the final numerical result, which is by 1.321% different from the theoretical J-integral value. A stress intensity

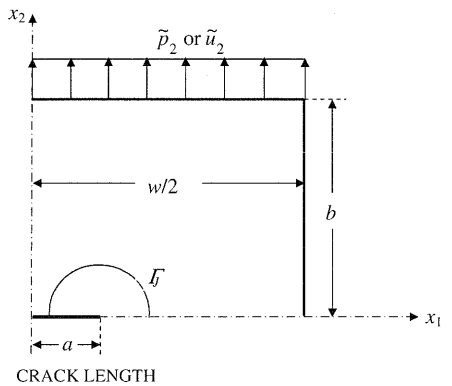

Fig. 2. Typical geometry and loading of analysed plates.

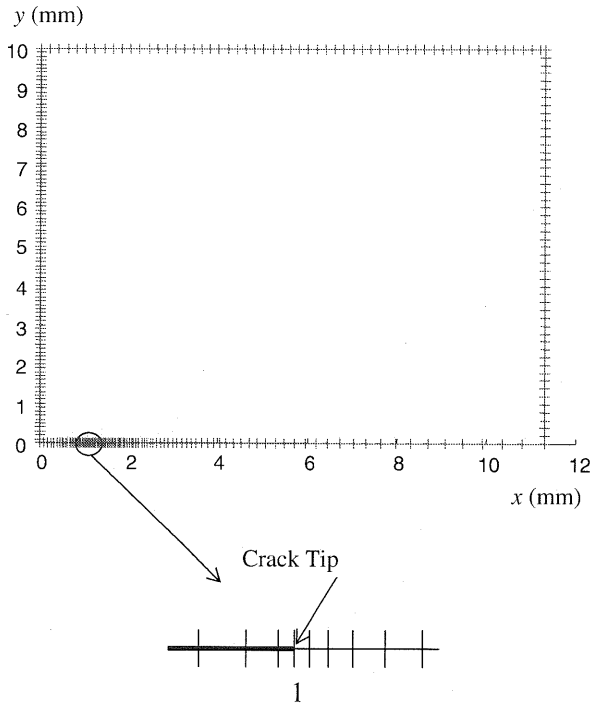

Fig. 3. Final boundary element mesh for the plate under constant tension.

factor of 18.0116 N/mm$^{3/2}$ was found directly from the stress field through a limiting process according to Eq. (5); this is by 1.291% greater than the theoretical solution. The stress intensity factor obtained from the elastic equivalent to Eq. (8) was 17.8991 N/mm$^{3/2}$; this differs from the theoretical K_I by only 0.658%. The adopted BEM modelling was thus shown to provide elastic fracture parameters with satisfactory accuracy and could be used with confidence in the subsequent viscoelastic applications.

4. Results

4.1. Centre-cracked plate under constant tension

The geometry, the loading, the constraints as well as the mesh of the model were exactly the same as those of the elastic problem described in the previous section. Under constant load, the plate deformation can be described as creep. The material behaviour was characterised by a shear relaxation modulus

$$\mu(t) = 23.625 + 70.875e^{-0.4t}\ (\text{GPa,s}). \tag{26}$$

Results were obtained by both the Laplace transform and direct time-domain boundary element formulations. The inverse transforms were calculated using 30 distinct values of the transform parameter s, with $s_1 = 0.001$ and $s_{i+1}/s_i = 2$ for $i = 1, \ldots, 29$.

Initially, a constant Poisson's ratio $v = 0.1$ was adopted. For such viscoelastic material behaviour, constant traction $\tilde{p}_i$ generates a constant stress field. Hence, the stress intensity factor is also constant. This was confirmed by BEM results from both the time-domain formulation using Eq. (5) and that based on Eqs. (7) and (8) and the BEM output from the Laplace transform domain formulation, under both plane strain and plane stress conditions. These stress intensity factors were found in excellent agreement with the analytical solution, the maximum differences being less than 1.25%.

Under creep conditions and constant v, p_2 is also constant and Eq. (14) gives

$$u_2(t') = C(r,t')p_2 \tag{27}$$

that is, a linear relationship between displacement and traction. As a result, Eq. (12) reduces to

$$G(a,t)\delta a = \int_0^{\delta a} p_2(r)u_2(r,t')\mathrm{d}r; \tag{28}$$

therefore, $G(a,t)$ increases with t. Eq. (28) implies correspondence with the behaviour of an elastic material with moduli $\mu(t')$ and $K(t')$ so that its left-hand side can be obtained from Eq. (11), which reduces in this special case to

$$G(a,t)\delta a = \frac{1}{2}\int_{\Gamma_p} \tilde{p}_i \delta u_i(t)\mathrm{d}\Gamma, \tag{29}$$

thus providing the strain energy release rate at any time $t > t_1$ during the viscoelastic response of the polymer.

A $J(t)$ integral equivalent to $G(t)$ can also be defined in the case of a constant traction (creep) experiment according to Eq. (18) with u_i^R and ε_{ij}^R taken as the actual displacements and strains at time t. It is evident from Eq. (16) that $G(a,t_1)$ is constant under creep conditions. This also true for $J(t_1)$ since, in this case, u_i^R and ε_{ij}^R are simply the initial elastic displacements and strains.

BEM predictions of $J(t)$ with $t_1 = 0$, from both time-domain and Laplace transform formulations under plane strain are plotted in Fig. 4 together with the corresponding analytical solution obtained by applying the correspondence principle. It can be seen that the results are almost identical for any time t. The same accuracy was achieved in the plane stress case. The energy release rate G was also calculated using both Eqs. (28) and (29) and found in very good agreement with the predicted J-integral.

The same problem was solved again but assuming that the material has a time-dependent Poisson's ratio for which the separation of variables conditions are not strictly applicable. Adopting instead a constant bulk modulus k of 86.625 GPa led to

$$\nu(t) = 0.375 - 0.275\mathrm{e}^{-0.32t} \tag{30}$$

obtained from the second of Eqs. (9) by Laplace transform inversion.

The boundary element formulation was first tested against the exact analytical solution for the crack-opening displacement, which is obtained from the respective elastic solution via the application of the correspondence principle. The BEM results under plane strain conditions, for a number of discrete times, were in excellent agreement with the theoretical predictions as can be seen by referring to Fig. 5.

The stress intensity factor was then calculated by the time-domain BEM using the limited process indicated by Eq. (5); it was also obtained from Eqs. (7) and (8), which require BEM output from the Laplace transform domain solution. The results, for plane strain conditions, are plotted in Fig. 6 together with an analytical solu-

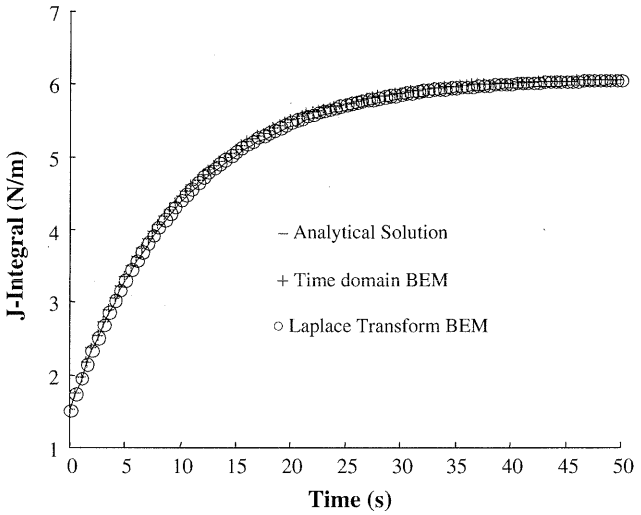

Fig. 4. J-integral for the centre-cracked specimen with constant Poisson's ratio under creep loading.

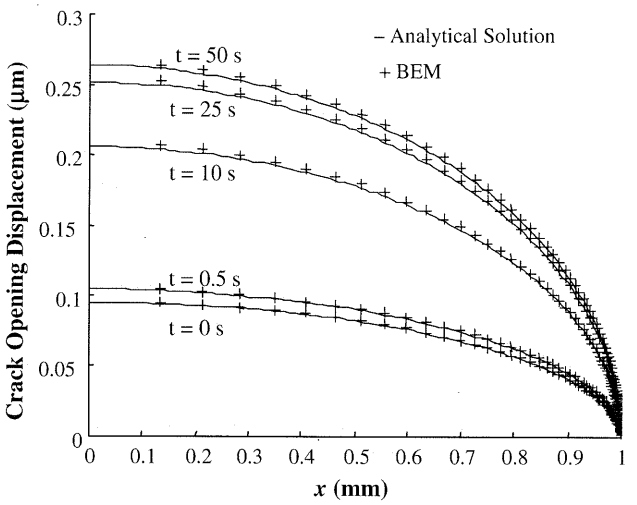

Fig. 5. Crack-opening displacement for the centre-cracked specimen with time-dependent Poisson's ratio under creep loading.

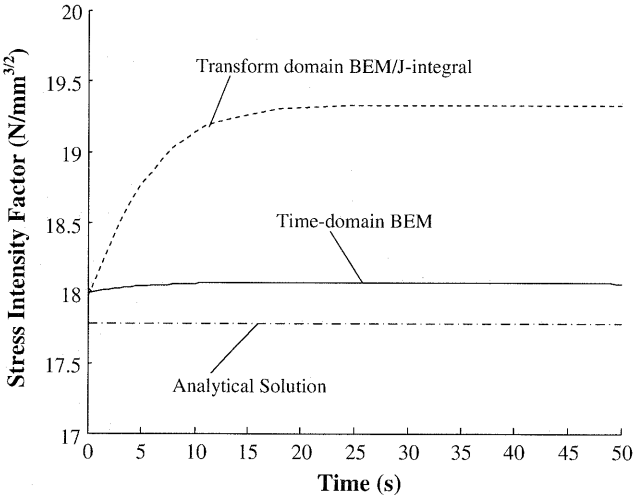

Fig. 6. Stress intensity factor for the centre-cracked specimen with time-dependent Poisson's ratio under creep loading.

tion based on the correspondence principle. The weak initial time-dependence of K_I obtained from the time-domain BEM is due to the time-dependence of Poisson's ratio. The other two methods of solution are based on the assumption of constant K_I under creep conditions; this explains the differences between their predictions and the time-domain BEM result. The three analyses were repeated under plane stress conditions and the differences between the corresponding steady-state K_I predictions were less than 1.5%. This better agreement can be attributed to the weaker dependence of K_I on the Poisson's ratio in the case of plane stress.

The J-integral was numerically evaluated by the same methods as those applied in the constant-ν case. An analytical solution was also obtained based on the correspondence principle. All three approaches entail a theoretical error, therefore, the observed discrepancies in the results were expected and there was no basis for meaningful comparison. As with the K_I results, these differences were considerably more severe in the case of plane strain analysis.

4.2. Long strip with centre crack under constant strain

The analysis was applied to a strip, which had been subjected to a range of loads at various temperatures to determine the corresponding crack propagation velocities [16]. The dimensions of the tested specimen were

adopted, that is, depth $2b = 34.925$ mm and length $w = 254$ mm. The thickness of the specimen was only 0.8 mm, therefore, plane stress conditions were applicable. The material was Solithane 50/50 for which the experimentally determined relaxation modulus at 0 °C was provided. Fitting exponential series to these data and assuming a constant Poisson's ratio $v = 0.5$ for the material, the shear relaxation function

$$\mu(t) = 1.33516 + 11.58289\mathrm{e}^{-63.891t} + 30.48149\mathrm{e}^{-956.825t} + 46.86602\mathrm{e}^{-16287.624t} + 50.76678\mathrm{e}^{-195553.092t}\ (\mathrm{MPa, s}) \tag{31}$$

was obtained. This corresponds to a glassy modulus $E(0) = 423$ MPa and a rubbery modulus $E(\infty) = 4$ MPa. The rapid decay of the relaxation modulus represented by Eq. (31) is consistent with the material description in Ref. [16]. A centre crack of length $2a = 60$ mm was assumed. Due to the symmetry of the problem, only one quarter of the strip was modelled as indicated in Figs. 2 and 3 using 154 'constant' elements. The elements on either side of the tip had a length of 0.002 mm. A constant displacement $\tilde{u}_2 = 1.746$ mm was applied at $y = 17.46$ mm; this corresponds to a nominal strain of 0.1 in the direction normal to the crack.

In this relaxation test, no further external work is done on the solid as a consequence of crack extension since $\delta u_i^{\mathrm{R}} = 0$ and Eq. (17) yielding the energy release rate $G(a,t_1)$ is reduced to

$$G(a,t_1)\delta a = -\frac{1}{2}\int_{\Gamma} \delta p_i u_i^{\mathrm{R}} \mathrm{d}\Gamma \tag{32}$$

It is clear from Eqs. (16) and (32) that $G(a,t_1)$ decreases under relaxation conditions. It is also evident from Eq. (11) that no further strain and dissipated energy is stored, hence $G(a, t')$ is constant for $t \geqslant t_1$.

The instantaneous elastic energy release rate $G(t_1)$ was obtained using both Eqs. (16) and (32) and a crack growth $\delta a = 0.002$ mm, that is, the length of a single element. The energy release rate was calculated as the work rate due to crack opening at the tip, Eq. (16); as the rate of potential energy loss, Eq. (32) and as the path independent J-integral defined through Eq. (18). The numerical process begins with the viscoelastic time-domain solution providing $p_i(t_1)$ over Γ and $p_2(t_1)$ over δa for any time t_1; these two sets of results become inputs to two elastic analyses, the former with the original and the latter with the extended crack. The elastic constants are the initial values of the relaxation moduli. The first of the two elastic analyses yields directly the J-integral as well as u_i^{R} over Γ; the second yields δp_i over Γ and δu_2 over δa. Fig. 7 shows that the results obtained by all three approaches are in excellent agreement, the maximum difference between predictions being less than 0.5%. This is remarkable considering that the integration in Eq. (16) was performed over a single element while the J-integral was evaluated by dividing the 5 mm-radius path into 18 segments.

4.3. Strip under constant strain rate

Again, due to the symmetry of the problem, only one quarter of the strip was modelled as indicated in Figs. 2 and 3. The boundary was divided into 131 elements with the minimum element length of 0.001 mm on either

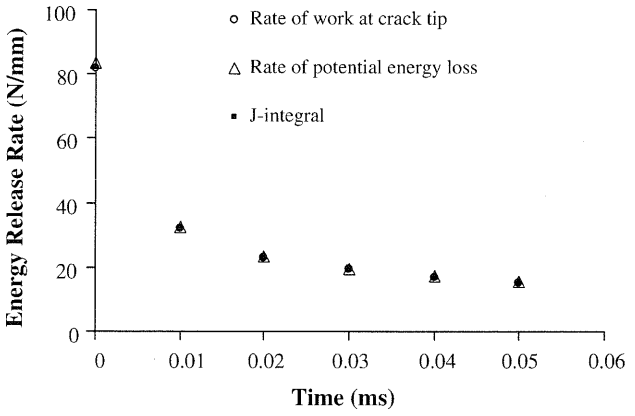

Fig. 7. Strain energy release rate for the specimen under constant strain.

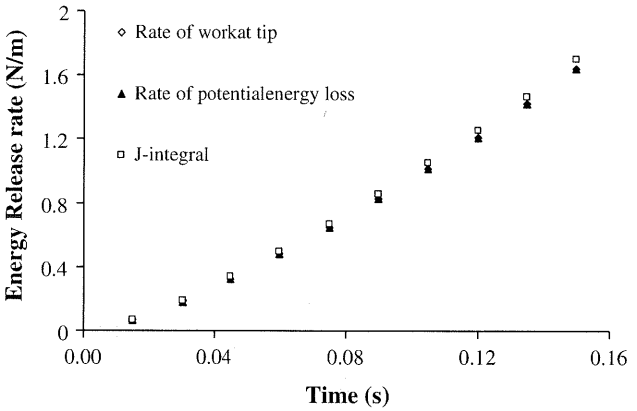

Fig. 8. Strain energy release rate for the specimen under constant strain rate.

side of the crack tip. The analysis was performed with a centre crack of half-length $a = 10.7$ mm, under plane stress conditions. The geometry was similar to that of Gutierrez-Lemini's specimen [25], that is, with a width w of 10.7 mm and a half-depth b of 19.2 mm. A Prony series was fitted to a given, rapidly decaying, tensile relaxation modulus, normalised with respect to $E(\infty)$ [25]. Adopting a constant Poisson's ratio of 0.496, led to the shear relaxation modulus

$$\mu(t) = 0.46789 + 1.28964e^{-19.9267t} + 2.93462e^{-1606.3t} + 5.86873e^{-34711.7t} \text{ (MPa, min)} \tag{33}$$

A displacement $\tilde{u}_2(t)$ was applied to the side $x_2 = b$ at the constant rate of 50 mm/min with a zero displacement at $t = 0$.

The rate of work at the crack tip was again calculated from Eq. (16) assuming a crack growth $\delta a = 0.002$ mm, the integration was therefore performed over two elements. Since this model simulates a displacement-controlled test, $\delta u_i^R = 0$ and $G(t_1)$ could also be obtained using Eq. (32) with u_i^R generated by elastic analysis of the plate with the original crack and shear modulus $\mu(0)$, subjected to the viscoelastic solution $p_i(t_1)$. The same analysis generated ε_{ij}^R and $u_{i,1}^R$ necessary for the evaluation of $J(t_1)$ using Eq. (18). Comparing the results from the three approaches shown in Fig. 8, the agreement between them can be considered satisfactory.

5. Discussion

In the special case of constant tension and Poisson's ratio v, the viscoelastic problem is greatly simplified since it is equivalent to a sequence of elastic problems with the current relaxation moduli values as elastic constants. Both time-dependent strain energy release rate G and J-integral account for energy dissipation and can be obtained with high accuracy. If v is not constant, the stress intensity factor K_I should be calculated by the time-domain approach, which takes into account its time-dependence. When the latter is ignored, the K_I, G and J-integral values calculated by various methods are inconsistent and such discrepancies are more significant in the case of plane strain.

Since the time-dependence of K_I under constant load is only due to the Poisson effect, it decays very quickly, therefore, this parameter is not a reliable representation of the material's fracture resistance. In contrast, the time-dependence of the energy release rate G is clearly identified whatever the loading conditions. This is also true for a properly defined J-integral in certain special cases. Therefore, the failure criterion in a viscoelastic fracture problem should be linked to the critical values of such parameters, that is, G_C or J_C.

In the case of instantaneous crack extension, that is, in the absence of energy dissipation, the problem of evaluating G or the J-integral reduces to an equivalent elastic one with the current viscoelastic solution for boundary traction and the initial values of the relaxation functions as the essential input. The consistency of the results obtained confirmed the validity of the adopted approaches but also the robustness of the BEM modelling despite its apparent simplicity.

When energy dissipation contributes to the energy release rate, the latter can only be determined as the work done at the tip of the extended crack. Then the analysis process becomes computationally more demanding since a second incremental viscoelastic solution, relying on the output of the first, is required for the determination of the rate of crack-opening displacement. This result can be used to evaluate also the crack propagation velocity c in the case of a non-stationary crack. It became obvious from the various modelling data of the previous section that a fine tuning between element length at the crack tip and time step size Δt in the BEM time-domain algorithm may be necessary to achieve a prediction of c with satisfactory accuracy and efficiency. This is because the former imposes a lower bound on the initial choice of δa, while Δt could be orders of magnitude smaller than the duration δt of the $p_2(r,t)$ time-history required for the integral on the right-hand side of Eq. (20) to balance the left-hand side. The problem can be addressed by adopting a time-step integration algorithm with variable Δt as indicated in Ref. [19]. The BEM time-domain algorithm thus needs to be sufficiently versatile to cope with the high initial time gradients of the material input and still provide both short and long term responses. Ideally, such numerical results should be obtained in parallel with experimental measurements for comparison and validation purposes.

6. Conclusions

BEM was shown to be a versatile numerical tool for generating key fracture parameters based on various formulations and analytical models. The agreement between BEM output obtained by various approaches was found satisfactory confirming the reliability of the method. Another general observation from the numerical results was that the results from time-domain BEM were more accurate than those obtained from the analysis in the Laplace transform domain. The additional numerical error can be attributed to the Laplace transform inversion required by the latter formulation. The time-domain formulation is also far more versatile in generating time-dependent energy release rates and for this reason it was exclusively used in the last two examples.

The presented formulation can be further adapted to the analysis of bi-material viscoelastic solids with cracks along their interfaces. This would require more general modelling schemes, which are applicable to problems with geometric, material or loading asymmetry. As with elastic fracture problems, a natural extension of the method would be towards including viscoelastic nonlinearity arising from the stress singularity at the crack tip. Based on an earlier finite element modelling of this effect [26], the present BEM time-domain formulation can be complemented with an irreducible domain integral depending on the volumetric strain. This integral would be accounted for through an iterative scheme within each step of the incremental solution process.

References

[1] Christensen RM. Theory of viscoelasticity: an introduction. New York: Academic Press; 1971.
[2] Schapery RA. On some path independent integrals and their use in fracture of nonlinear viscoelastic media. Int J Fract 1990;42:189–207.
[3] Rice JR. A path independent integral and the approximate analysis of strain concentration by notches and cracks. J Appl Mech-Trans ASME 1968;35:379–86.
[4] Schapery RA. A theory of crack initiation and growth in viscoelastic media I. Theoretical development. Int J Fract 1975;11:141–59.
[5] Schapery RA. A theory of crack initiation and growth in viscoelastic media-II. Approximate methods of analysis. Int J Fract 1975;11:369–88.
[6] Schapery RA. A theory of crack initiation and growth in viscoelastic media-III. Analysis of continuous growth. Int J Fract 1975;11:549–62.
[7] Christensen RM, Wu EM. A theory of crack growth in viscoelastic materials. Engng Fract Mech 1981;14:215–25.
[8] Knauss WG. The mechanics of polymer fracture. Appl Mech Rev 1973;26:1–17.
[9] Mackerle J. Finite-element analysis and simulation of polymers: a bibliography. Model Simul Mater Sci Engng 1997;5:615–50.
[10] Sladek J, Sumec J, Sladek V. Viscoelastic crack analysis by the boundary integral-equation method. Ingenieur Archiv 1984;54:275–82.
[11] Sun BN, Hsiao CC. Viscoelastic boundary element method for analysing polymer quasifracture. Comput Struct 1988;30:963–6.
[12] Lee SS, Kim YJ. Time-domain boundary element analysis of cracked linear viscoelastic solids. Engng Fract Mech 1995;51:585–90.
[13] Syngellakis S, Wu J. Boundary element applications to polymer fracture. In: Brebbia CA, Poljak D, Roje V, editors. Boundary elements XXV. Southampton: WIT Press; 2003. p. 83–92.
[14] Nilsson F. A path-independent integral for transient crack problems. Int J Solids Struct 1973;9:1107–15.
[15] Atkinson C, Craster RV. Theoretical aspects of fracture mechanics. Prog Aerosp Sci 1995;31:1–83.

[16] Mueller HK, Knauss WG. Crack propagation in a linearly viscoelastic strip. J Appl Mech-Trans ASME 1971;38:483–8.
[17] Williams JG. Fracture mechanics of polymers. Chichester: Ellis Horwood; 1984.
[18] Syngellakis S. Boundary element methods for polymer analysis. Engng Anal Bound Elem 2002;27:125–35.
[19] Syngellakis S, Wu JW. Evaluation of various schemes for quasi-static boundary element analysis of polymers. Engng Anal Bound Elem 2004;28:733–45.
[20] Schapery RA. Approximate methods of transform inversion for viscoelastic stress analysis. In: Rosenberg RM, editor. Proceedings of the fourth US national congress of applied mechanics. New York: ASME; 1962. p. 1075–85.
[21] Cruse TA. Two-dimensional BIE fracture mechanics analysis. Appl Math Model 1978;2:287–93.
[22] Gurtin ME, Sternberg E. On the linear theory of viscoelasticity. Arch Ration Mech Anal 1962;11:291–356.
[23] Brebbia CA, Walker S. Boundary element techniques in engineering. London: Butterworth; 1980.
[24] Aliabadi MH, Cartwright DJ, Rooke DP. Fracture-mechanics weight-functions by the removal of singular fields using boundary element analysis. Int J Fract 1989;40:271–84.
[25] Gutierrez-Lemini D. The initiation J-integral for linear viscoelastic solids with constant Poisson's ratio. Int J Fract 2002;113:27–37.
[26] Moran B, Knauss WG. Crack-tip stress and deformation fields in strain-softening nonlinearly viscoelastic materials. J Appl Mech-Trans ASME 1992;59:95–101.